Scalable Electrochemical FET Immunosensor with Crumpled Graphene for Sensitive Detection of Prostate Cancer Derived Exosomes

Piyali Mukherjee[a], Naresh Bahadursha[b], Nahid Sultana[c], Usha Rani Dash[a], Pratyusha Chikkala[d,e], Sayan Kanungo[b*], Sanghamitra Sengupta[c*], Chirasree RoyChaudhuri[a*]

Supplementary Information

S1 Electrokinetic Simulation

The capture of exosomes can be significantly enhanced by applying AC electric fields, which induce external forces such as dielectrophoresis (DEP) and AC electroosmotic (ACEO) flow. In this work, an AC electric field is applied between the gate and the shorted drain-source electrodes (to prevent any drain-source current through graphene) when the analyte containing exosomes is introduced onto the sensor surface. During this process, the gate bias is kept off to avoid any shift in the device operating point. In an electrolyte medium, both the sensing surface and electrodes are surrounded by an electrical double layer (EDL), and the interaction of ions within this layer with the tangential component of the applied electric field generates ACEO flow. Simultaneously, DEP governs the motion of polarizable particles in a non-uniform electric field through the interaction of induced dipole moments with the external field. Depending on their polarizability, particles migrate toward regions of higher electric field (positive DEP, p-DEP) or lower electric field (negative DEP, n-DEP) to minimize electrostatic energy. In the absence of such field-induced forces, exosome transport is predominantly diffusion-limited. For an initial analyte concentration C_0, the time required to accumulate n particles on a circular electrode of radius a follows $t(n) = \frac{n}{4DC_0a}$, where D is the diffusion coefficient[1]. This relation suggests that for low concentrations (e.g., 1000 particles/ml), adsorption of even a single exosome onto a ~100 µm electrode may take several hours. Therefore, the combined action of DEP and ACEO is critical for accelerating analyte transport and enhancing surface capture. Initially, ACEO is employed to drive particles from the bulk solution toward the sensing interface. At low frequencies, the time-averaged Maxwell stress induces fluid motion from electrode edges toward the center, producing an electroosmotic slip velocity described by the Helmholtz–Smoluchowski relation (1):

$$\langle u_s \rangle = \frac{-\epsilon_m}{4\eta} \Lambda \frac{\partial}{\partial x} |\phi - V|^2 \quad (1)$$

where, Λ represents the ratio of potential drop across the diffuse layer to the total double layer[2] (assumed ~0.5), ϕ is the potential at the outer Helmholtz plane, and V is the applied voltage. ϵ_m and η denote the permittivity and viscosity of the medium, respectively. A 2 V peak-to-peak sinusoidal signal with frequency sweep from 1 to 10 kHz has been applied to induce ACEO. Finite element simulations (COMSOL Multiphysics 6.0), using a simplified hemispherical approximation of the crumpled morphology, reveal that ACEO effectively transports particles toward the surface and concentrates them at the sensing region.

To determine the optimal operating condition, coupled ACEO-DEP simulations were performed. The DEP force acting on a spherical particle is given by equation 2:

$$F_{dep} = 2\pi r_p^3 \varepsilon_0 real(\varepsilon_p^*) real\left(\frac{\varepsilon_p^* - \varepsilon_m^*}{\varepsilon_p^* + 2\varepsilon_m^*}\right) \nabla |E_{rms}|^2 \quad (2)$$

where r_p is the particle radius, ϵ_0 is the vacuum permittivity, and $\epsilon_p{}^*$, $\epsilon_m{}^*$ are the complex permittivities of the particle and medium, respectively. The complex permittivity is expressed as:

$$\varepsilon^* = \varepsilon - \frac{i\sigma}{\omega}$$

with ϵ, σ and ω denoting permittivity, conductivity and angular frequency. The DEP response is governed by the Clausius–Mossotti (CM) factor, which is $real\left(\frac{\varepsilon_p^* - \varepsilon_m^*}{\varepsilon_p^* + 2\varepsilon_m^*}\right)$, that dictates whether particles experience p-DEP or n-DEP.

In the proposed sensor architecture, the channel area is smaller than the gate, leading to enhanced electric field intensity over the sensing region, thereby favouring p-DEP-based concentration. Further finite element analysis using a computationally efficient crumpled model shows that at 1 kHz, ACEO dominates due to weak DEP forces and at 10 kHz, DEP and ACEO act synergistically to concentrate particles near the center; (Fig. S1a). Based on this, 10 kHz has been selected as the optimal frequency, ensuring efficient enrichment for plasma samples from normal, benign and prostate cancer patients. Importantly, exosomes exhibit size heterogeneity (50-250 nm), and their physical properties, including effective dielectric constant vary accordingly. To account for this, the variation of the CM factor with frequency has been evaluated, which confirmed that at 10 kHz, the CM factor remains positive across the considered size range, ensuring consistent p-DEP-driven attraction toward high-field regions (Fig. S1b).

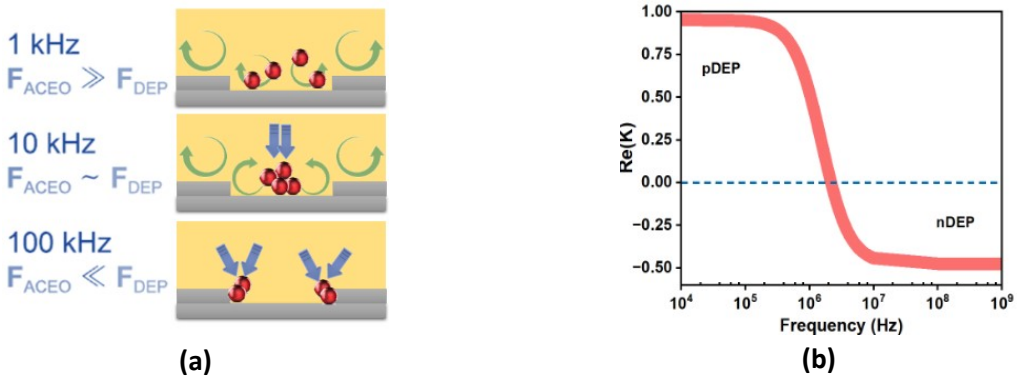

Fig. S1 (a) Schematic illustration of the particle-trapping mechanism under applied AC electric fields at frequencies of 1 kHz, 10 kHz (b) Variation of CM factor with frequency

S2. Effective Surface Area Computation

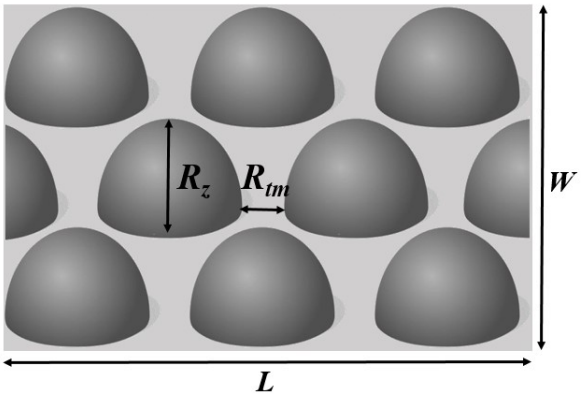

The effective surface area of the curved surface morphologies (surface A, B and C) has been calculated with respect to the surface area of the flat surface.

Let the surface area for the flat surface be ***L.W;*** where *L* is the length and *W* is the width of the rectangular surface.
Let R_z and R_{tm} be the height of the hemispheres and the spacing between two hemispheres respectively as depicted above.

Effective surface area for crumpled surface $= [LW + n\pi R_Z^2]$, where $n = \left[\frac{L.W}{(2R_Z + R_{tm})2R_Z}\right]$

Considering the values of R_{tm} and R_z from atomic force microscopy measurements, the effective surface area for surface A, B and C becomes 1.54, 1.52 and 1.45 times that of flat surface respectively.

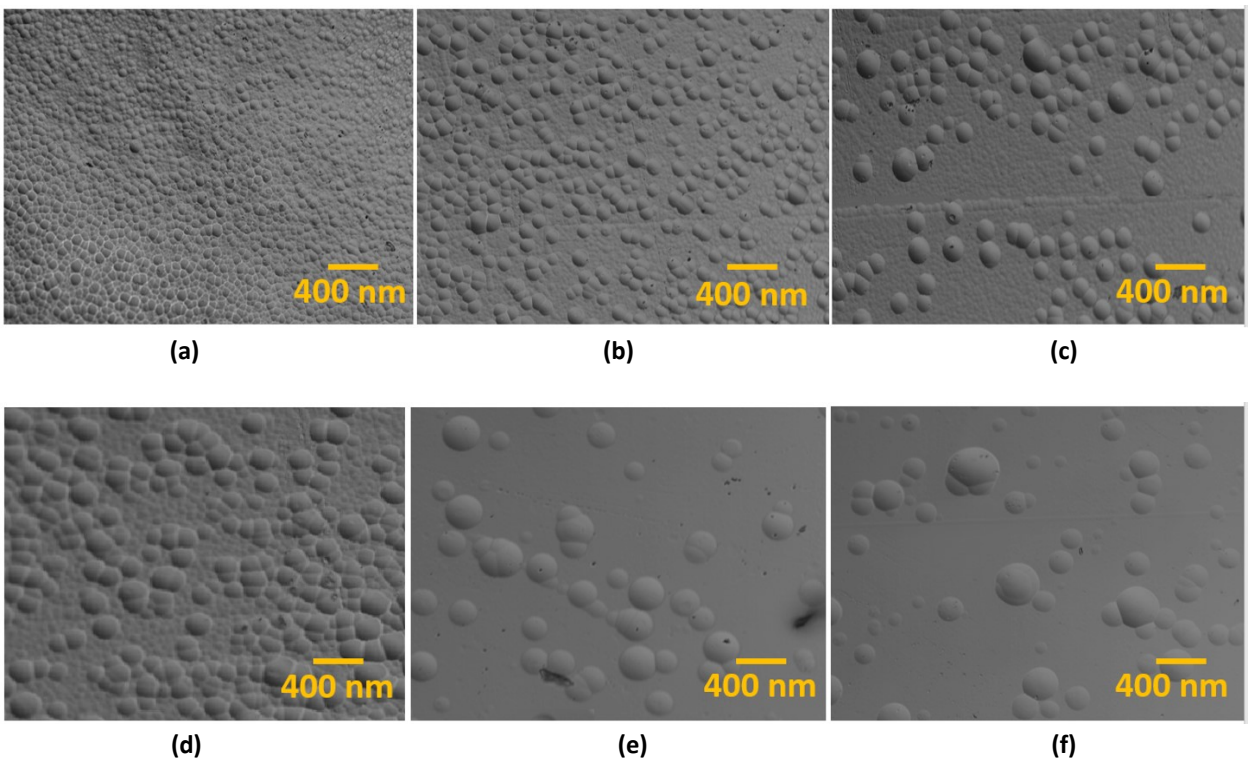

Fig. S2 (a-c),(d-f) SEM images of different morphologies owing to process parameter variations.

S3. Density Functional Theory Computation for Protein Adsorption on Crumpled Graphene

In this work, typical protein interaction on the flat (F) and undulated (U) graphene (Gr) is modelled using density functional theory (DFT) based first principle simulation employing the Atomistix Tool Kit (ATK) and Virtual Nano Lab (VNL) software suite, commercially available from Synopsys QuantumATK[3]. For DFT simulation, a Linear Combination of Atomic Orbitals (LCAO) PseudoDojo basis set is considered with an energy cutoff of 125 Hartree, and a 2 × 2 × 2 Monkhorst-Pack k-point mesh for Brillouin zone sampling. The F-Gr and U-Gr structures, as well as their corresponding Gr-protein binding systems, are relaxed by geometry optimization using the Limited memory Broyden Fletcher Goldfarb Shanno (LBFGS) algorithm, with convergence criteria set to 0.01 eV/Å for forces per atom and 0.0001 eV/Å^3 eV for pressure per atom. For geometry optimization and energy calculation the Generalized Gradient Approximation (GGA) with the Perdew–Burke–Ernzerhof (PBE) exchange-correlation functional is considered with Grimme's DFT-D3 dispersion correction[4] for incorporating van der Waals (vdW) interactions in Gr-protein binding systems.

Next, to reliably model the U-Gr structures as well as protein interactions at different morphological sites, a 10×10×1 supercell of Gr is considered by repeating the unit cell in in-plane directions (Fig. S3a). The U-Gr structure is modelled by bending the F-Gr along one in-plane crystalline axis direction with specific curvature, which is determined from the ratio of the height (separation between the top and bottom C atoms along the out-of-plane direction) and width (separation between the top and bottom C atoms along the in-plane direction). The two different undulation curvatures of U-Gr, i.e., width-height ratio of 2 and 1.05, are considered for theoretical modelling, corresponding to the experimentally synthesized U-Gr in this work (Fig. S3b and S3c).

In this work, the strength of protein (cysteine has been considered for simplicity) adsorption on F-Gr and U-Gr can be quantified from the adsorption energy (E_{ads}), wherein the strength of transduction can be quantified from the charge transfer (Q_{trans}).

The E_{ads} is defined as follows[5]:

$$E_{ads} = E_{Gr+Cys} - (E_{Gr} + E_{Cys}) \quad (3)$$

In **equation 3**, E_{Gr+Cys} represents the total energy of the graphene-cysteine system, E_{Gr} is the energy of the relaxed graphene substrate (either F-Gr or U-Gr), and E_{Cys} denotes the energy of the isolated cysteine molecule in vacuum. The Q_{trans} is calculated using the Mulliken charge analysis and is defined as follows[5]:

$$Q_{trans} = Q_{Cysteine\_before\_adsorbtion} - Q_{Cysteine\_after\_adsorbtion} \quad (4)$$

In **equation 2**, $Q_{Cysteine\_before\_adsorbtion}$, and $Q_{Cysteine\_after\_adsorbtion}$ are the total charge of cysteine before and after adsorption on F-Gr and U-Gr, respectively. It should be noted that the E_{ads} < 0 indicates a stable system, and the magnitude of E_{ads} indicates the strength of cysteine/Gr interactions. Similarly, Q_{trans} < 0 (Q_{trans}> 0) indicates electrons are transferred from Gr to cysteine (from cysteine to Gr), which corresponds to acceptor-type (donor-type) charge transfer.

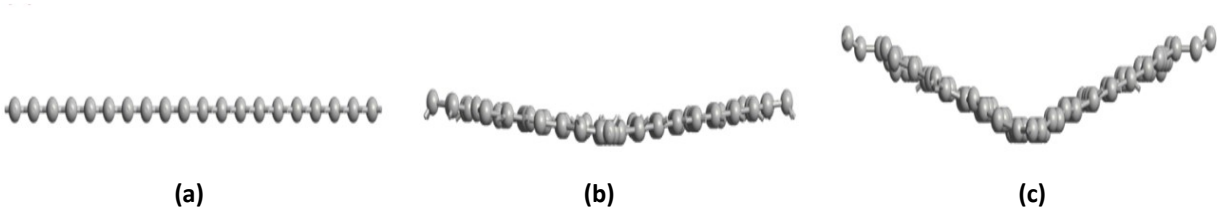

Fig. S3 Schematic representations of (a) F-Gr, (b) U-Gr (height: width = 2: 2) and (c) U-Gr (height: width = 1:1.05).

To theoretically analyse the influence of undulation in graphene (Gr) on the adsorption behaviour of cysteine, the cysteine adsorption on both flat graphene (F-Gr) and undulated graphene (U-Gr) surfaces is considered at different molecular orientations of cysteine and different morphological sites of U-Gr for an ab initio DFT study. The use of L-cysteine as a model molecule in the DFT simulations is not intended to replicate the entire biochemical complexity of an exosome; rather, it serves as a molecular proxy to elucidate the fundamental charge-surface interaction mechanism governing biomolecular adsorption on the crumpled rGO surface. Exosomes are nanoscale vesicles comprising thousands of lipids, proteins, and surface glycol-conjugates in their single representative units. Hence, a direct DFT treatment of an entire exosome-graphene interface will require large supercell of undulated graphene which is computationally extremely challenging. Cysteine has been chosen because it contains key functional groups (–NH_2, –COOH, and –SH) that are chemically analogous to the amino acid and thiol residues present in exosomal membrane proteins and extracellular vesicle surface markers. These groups are known to engage in hydrogen bonding, dipole interactions and charge transfer with graphitic surfaces, the same classes of interactions that govern exosome-sensor coupling at the molecular scale. The goal of the DFT study is to reveal how nanoscale curvature and hybridization gradients in crumpled graphene influence local adsorption energy and electronic structure phenomena that are scale-independent and molecule-agnostic. Although cysteine is small, its dipolar and polarizable groups capture electronic coupling behaviour faithfully, allowing quantification at curved vs. flat regions. Thus, cysteine is used as a representative molecular probe to reveal how graphene's topological modulation alters charge transfer dynamics, not to model the full biomolecular complexity of exosome binding.

The results indicate that in general, cysteine exhibits physisorption (E_{ads} > -1 eV) on both F-Gr and U-Gr surfaces. Specifically, in both stable configurations of F-Gr, the oxygen of cysteine is pointed towards the surface (Fig. S4(a-b)), which exhibits relatively smaller E_{ads} (-0.50 eV), consistent with a marginal Q_{trans} (-0.002 e^-). The undulation in Gr compromises the planar structure and thereby distorts sp^2 hybridization and π-π electron clouds, suggesting a notable change in surface chemistry in U-Gr compared to that of F-Gr. The local electron distributions on the U-Gr surface and thereby electrostatic interactions between the U-Gr and adsorbed molecule depend on the degree of undulation as well as the direction of curvature, i.e., concave or convex configurations. Consequently, the cysteine is horizontally aligned on the concave sites of U-Gr (Fig. S4(c) and (e)), whereas it is vertically pointing towards the convex site of U-Gr (Fig. S4(d)). In general, at the concave and the convex sites of U-Gr, the E_{ads} and Q_{trans} increase compared to F-Gr (Fig. S3(c)-(e)). Specifically, for the moderate curvature (height: width = 1:2) in U-Gr, the highest E_{ads} (-0.66 eV) is observed on the concave side (Fig. S4(c)), wherein a slightly smaller E_{ads} (-0.63 eV) is observed on the convex side (Fig. S4(d)). In contrast,

at a higher undulation curvature (height: width = 1:1.05), a slightly smaller E_{ads} (-0.61 eV) is observed on the concave side (Fig. S4(e)). Interestingly, a notable donor-type Q_{trans} (+0.014 e^-) is observed at the convex side (Fig. S4(d)) of the moderately undulated Gr, compared to negligible Q_{trans} (< |0.005| e^-) in all other cases of F-Gr and U-Gr. These results demonstrate that the surface morphology of Gr has a notable influence on the strength of cysteine interaction on Gr. On flat graphene, adsorption is weak and characterized by minimal charge transfer, indicating physisorption interactions with cysteine acting as a slight electron acceptor. However, the relationship between curvature and E_{ads} is not linear, suggesting that atomic environment and molecular orientation also play crucial roles. In essence, the theoretical study indicates that undulation (crumple) on Gr surface increases the strength of protein interaction on Gr surface, which in conjunction with the reduced Debye screening, may lead to the experimental sensitivity improvement observed in this work.

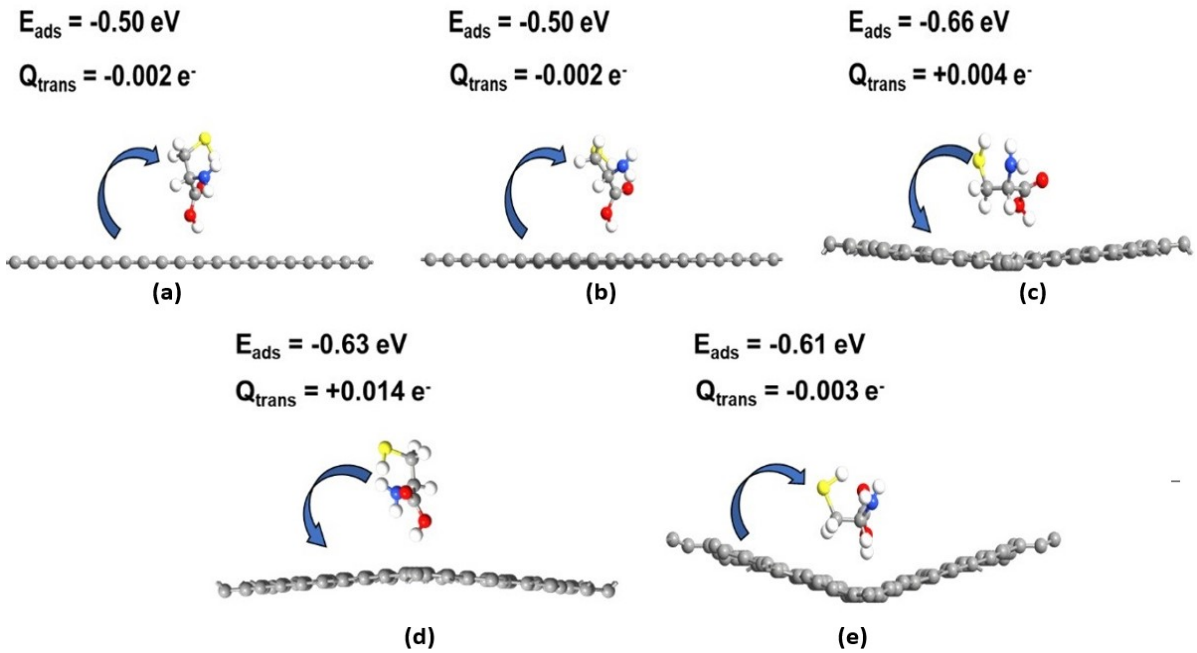

Fig. S4 Schematic representations of protein molecule interacting with modelled monolayer graphene configurations: (a) F-Gr, (b) F-Gr and (c) U-Gr (1:2), (d) U-Gr (1:2) and (e) U-Gr (1:1.05).

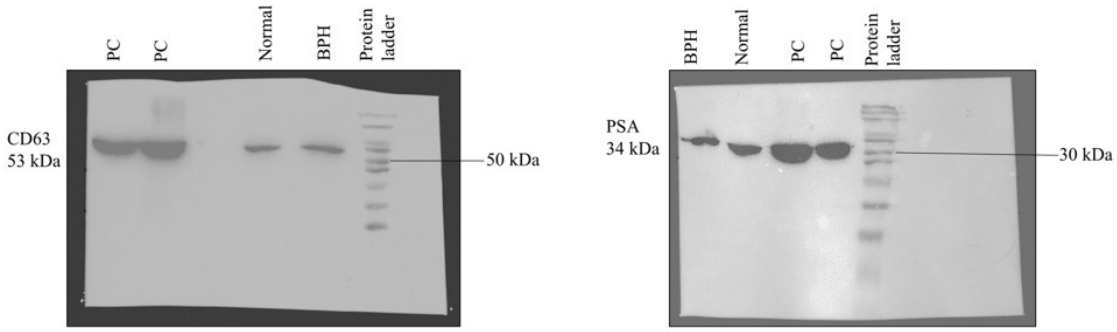

Fig.S5 Uncropped Western Blot Images

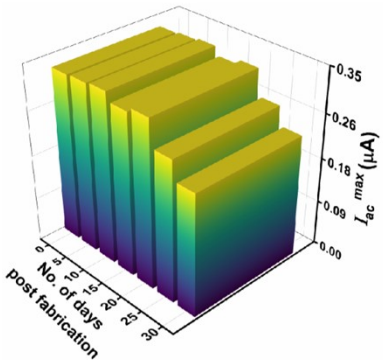

Fig. S6 Stability of the CD63 antibody immobilized sensor output as a function of time.

References:

1. Ibsen S.D., Wright J, Lewis J.M., *et al.* Rapid Isolation and Detection of Exosomes and Associated Biomarkers from Plasma, ACS Nano 2017, 11, 7, 6641–6651.
2. Wiegerinck H.T.M, Wood J.A., Eijkel J.C.T., Lammertink R.G.H, Frankel I, Ramos A. Continuous Focusing of Particles by AC-Electroosmosis and Induced Dipole Interactions, Langmuir 2024, 40, 19988-19996,.
3. QuantumATK version 2021.06, Synopsys QuantumATK [Online]. Available: https://quantumwise.com/
4. Grimme S. Semiempirical GGA-type density functional constructed with a long-range dispersion correction. Journal of computational chemistry. 2006 Nov 30;27(15):1787-99.
5. Tiwari A, Apte AA, Dyavadi SK, Balaji ES, Bahadursha N, Kanungo S. Surface engineered phosphorene using boron and arsenic doping/Co-doping for Co-optimizing the adsorption stability, transduction, and recovery of CO, NO, and SO gases–a density functional theory perspective. Materials Today Communications. 2023 Aug 1;36:106627.